Earth and Planetary Science Letters 410 (2015) 62–74

Contents lists available at ScienceDirect

Earth and Planetary Science Letters

www.elsevier.com/locate/epsl

An early solar system magnetic field recorded in CM chondrites

C. Cournede [a,*], J. Gattacceca [a,b], M. Gounelle [c,d], P. Rochette [a], B.P. Weiss [b], B. Zanda [c,e]

[a] Aix-Marseille Université, CNRS, CEREGE, UM34, Aix en Provence, France
[b] Department of Earth, Atmospheric and Planetary Sciences, Massachusetts Institute of Technology, Cambridge, MA 02139, USA
[c] IMPMC, Muséum national d'Histoire naturelle et Sorbonne Université, UPMC, CNRS UMR 7590, IRD UMR 206; Case Postale 52, 61 rue Buffon, F-75005 Paris, France
[d] Institut universitaire de France, 103 Bd St Michel, 75005 Paris, France
[e] IMCCE, Observatoire de Paris, 77 ave Denfert Rochereau, 75014 Paris, France

ARTICLE INFO

Article history:
Received 11 June 2014
Received in revised form 15 November 2014
Accepted 18 November 2014
Available online xxxx
Editor: B. Marty

Keywords:
meteorite paleomagnetism
CM carbonaceous chondrites
disk magnetic field
dynamo magnetic field

ABSTRACT

We present a paleomagnetic study of seven CM carbonaceous chondrites. CM chondrites are believed to be some of the most chemically primitive materials available in our solar system and may sample the continuum of transitional objects between asteroids and comets formed in the outer solar system. As such, CM chondrites can help us to understand primordial aspects of the history of the early solar system including protoplanetary disk and planetesimal magnetism.

The ferromagnetic assemblage of CM chondrites is composed of a mixture of primary metallic iron, pyrrhotite, and magnetite. The remanent properties are usually dominated by secondary pyrrhotite. Paleomagnetic analyses using thermal and alternating field demagnetization identified a stable origin-trending component of magnetization in the seven studied CM chondrites. In each meteorite, this component is homogeneous in direction at least at the cm scale and is therefore post-accretional. We interpret this stable component as a pre-terrestrial chemical remanent magnetization acquired during crystallization of magnetite and pyrrhotite during parent body aqueous alteration in a field of at least a few µT (2 ± 1.5 µT).

Considering the timescale and intensities of primordial magnetic fields, both internally generated fields from a putative dynamo and external fields, generated in the protoplanetary disk, may have been recorded by CM chondrites. It is presently difficult to discriminate between the two hypotheses. Regardless, CM chondrites likely contain the oldest paleomagnetic record yet identified.

1. Introduction

The study of the remanent magnetization (paleomagnetism) of extraterrestrial materials gives clues to the history of the primitive solar system and its evolution. Indeed, paleomagnetic studies of meteorites provide a unique window into understanding early solar magnetic fields within the solar protoplanetary disk itself as well as dynamo magnetic fields generated within the convecting metallic cores of planetesimals (e.g., Weiss et al., 2010). In this study we focus on CM carbonaceous chondrites, a meteorite group whose paleomagnetism has not been comprehensively analyzed.

CM chondrites are of particular interest because even though they represent only 1.5% of meteorites falls (Grady, 2000), CM-like materials represent a significant fraction of the micrometeorite flux (Gounelle et al., 2005a, 2005b). In addition, they are regarded as some of the most chemically primitive materials available in our solar system (Mason, 1962; Wood, 1963; Anders, 1971) and may be related to asteroids and/or comets (Aléon et al., 2009; Haack et al., 2011). They could have formed in the outer solar system (Wasson, 1976; Wasson and Wetherill, 1979; Gounelle et al., 2008). As such, they offer the possibility to estimate magnetic field strengths present in the early solar system.

1.1. CM chondrite petrography and petrogenesis

CM chondrites consist of chondrules, mineral and chondrule fragments, and calcium–aluminum inclusions (CAIs) embedded in a fine-grained matrix. These rocky components were accreted together with ice to form the CM parent-body (Young et al., 1999; Grimm and McSween, 1989). Following accretion, the ice melt and aqueous alteration took place on the parent body. This process generated alteration minerals such as phyllosilicates, carbonates, iron sulfides and iron oxides (Rosenberg et al., 2001; Brearley, 2006). A range of intensity of aqueous alteration has been observed

* Corresponding author.
E-mail address: cournede@cerege.fr (C. Cournede).

http://dx.doi.org/10.1016/j.epsl.2014.11.019

in CM chondrites (Browning et al., 1996; Rubin et al., 2007; Howard et al., 2011; Hewins et al., 2014).

Almost all CM chondrites are unshocked (classified as S1) (Scott et al., 1992). However, they are breccias that contain sub-centimeter size clasts whose degree of alteration is sometimes different (Rubin and Wasson, 1986; Alexander et al., 2010; Zanda et al., 2010; Jenniskens et al., 2012; Hewins et al., 2014). As such, it was proposed that aqueous alteration in CM may have been triggered by low intensity impacts (Rubin, 2012; Lindgren et al., in press). It is noteworthy that although some CM chondrites show evidence of thermal metamorphism likely generated by shock processes (Nakato et al., 2013), those considered here escaped heating above ∼40 °C (Guo and Eiler, 2007; Kimura et al., 2011).

The generally accepted view is that aqueous alteration of CM chondrites was a post-accretionary asteroidal process (e.g., McSween, 1979; Tomeoka et al., 1989; Hanowski and Brearley, 2000, 2001). However aqueous alteration in small precursor planetesimals prior to the formation of the CM parent asteroid is also advocated for some CM chondrites (Metzler et al., 1992; Bischoff, 1998; Lauretta et al., 2000). I–Xe dating indicates that magnetite in Murchison formed 2.4 ± 0.1 Ma after CAIs (Pravdivtseva et al., 2013). Carbonates in CM chondrites have also been dated using the Mn/Cr system. Because the solar system initial abundance of ^{53}Mn is poorly known, and because suitable carbonate standards are lacking, these ages are to be taken with caution. The most recent work indicates that carbonates in CM chondrites formed roughly 4 Myr after CAIs (Fujiya et al., 2012). Even if no firm timing constraints arise, it is clear that aqueous alteration occurred dominantly very early in solar system history, through a single event or episodic events over a period encompassing at least 2.4–4 million years (Myr) after CAI formation (Brearley, 2006; De Leuw et al., 2009).

Ejection of most CM meteorites from their parent body took place less than 2 Myr ago (e.g., Eugster et al., 2006).

1.2. CM magnetic properties: state of the Art

The magnetic properties of a dozen CM chondrites were studied previously (review in Weiss et al., 2010; Elmaleh et al., 2012). Although all CM chondrites are chemically similar, considerable differences exist in their mineralogy as illustrated by their ferromagnetic phases (Hyman and Rowe, 1983). The magnetic mineralogy of CM chondrites is composed, in various proportions, of metallic iron (<1.5 wt%), magnetite (<3 wt%), and iron–nickel sulfides (especially pyrrhotite, 0.7–3.1 wt%) (Hyman and Rowe, 1986; Burgess et al., 1991; Rochette et al., 2008; Howard et al., 2009). The magnetic susceptibility of CM chondrites varies by nearly two orders of magnitude (Rochette et al., 2008), indicating large variations in the magnetic mineral assemblage, abundance, and possibly grain size variations.

Magnetite in CM chondrites is a secondary mineral formed on the parent asteroid by oxidation of carbides and pyrrhotite (Brearley, 2003, 2011). Two populations of pyrrhotite may be distinguished in CM chondrites. A coarse grained (∼10 μm) pyrrhotite of primary origin, located in chondrules (Harries and Langenhorst, 2013; Brearley and Martinez, 2010), is present only in low abundance (<0.2 vol%). Secondary pyrrhotite nanoparticles are observed in the matrix and in the fine grained rims (Chizmadia and Brearley, 2008). This latter was formed on the CM parent body through aqueous alteration process. CM chondrites can also contain metal (Rubin et al., 2007; Hewins et al., 2014) and schreibersite (Nazarov et al., 2009).

The paleomagnetism of CM chondrites has been previously investigated (review in Weiss et al., 2010). These meteorites possess a natural remanent magnetization (NRM) (Banerjee and Hargraves, 1971). Partial alternating field (AF) demagnetization of four meteorites showed that this NRM is stable (Larson et al., 1973). The NRM was interpreted as a thermoremanent magnetization (TRM), thermochemical remanent magnetization (TCRM), or chemical remanent magnetization (CRM) (Banerjee and Hargraves, 1972; Larson et al., 1973). For Murchison, a minimum paleointensity of 20 μT was estimated with the Thellier–Thellier method (Banerjee and Hargraves, 1972). Much lower values of 0.2–2 μT were determined by non-heating methods (Kletetschka et al., 2003). From these previous studies, no clear picture regarding the nature of the NRM, and the nature and intensity of the magnetizing field has emerged.

Here, we performed a paleomagnetic study of seven CM carbonaceous chondrites: Banten, Cold Bokkeveld, Murchison, Murray, Mighei, Nogoya (falls), and Paris (fresh find). Unlike previous studies, we studied mutually-oriented subsamples, and used both AF and thermal demagnetization. We also evaluated the possibility of viscous remanent magnetization (VRM) and shock remanent magnetization for each meteorite, and discussed the time–temperature stability of the NRM. Our aim was to characterize their magnetic mineralogy, determine the nature and age of NRM, and estimate the intensity and nature of the paleofield.

2. Samples and methods

2.1. Samples

Samples of seven CM2 chondrites were supplied by the *Muséum national d'Histoire naturelle* (*Paris, France*) (list in Supplemental Table A). They collectively span a wide range of aqueous alteration (Browing et al. 1996; Rubin et al., 2007).

All samples were stored in a magnetically shielded room (field <400 nT) for at least one month to allow partial decay of the VRM acquired in the geomagnetic field since their fall. As the original orientations of the samples on the parent body are unknown, sample orientations were chosen arbitrarily. Samples were cut in mutually-oriented cubic subsamples using a diamond wire saw lubricated with ethanol. After cutting, we checked that the sum of the NRM of the sub-samples was consistent with the NRM of the original sample, indicating that no remagnetization was associated with sawing.

2.2. Magnetic measurements

Remanence measurements were performed with a 2G SQUID magnetometer (model 755R, noise level 10^{-11} A m^2) with an attached alternating field (AF) 3-axis demagnetization system. Thermal demagnetization was performed using an MMTD furnace, under argon atmosphere above 250 °C. Hysteresis measurements were performed at room temperature with a Princeton Micromag Vibrating Sample Magnetometer (VSM), and provided saturation remanent magnetization (M_{rs}), saturation magnetization (M_s) and the coercive force (B_c). The remanent coercive force (B_{cr}) was determined by back field experiments performed with the VSM. For most samples, we measured the S ratio that is the isothermal remanent magnetization (IRM) obtained after applying a 3 T field and then a back field of −0.3 T normalized to the IRM acquired in 3 T. Low temperature (40 to 180 K) experiments were carried out using the VSM and a Quantum Design Magnetic Properties Measurements System (MPMS).

The low field specific susceptibility (χ in m^3 kg^{-1}) and its anisotropy were measured using Agico MFK1 apparatus operating at 976 Hz and 200 A m^{-1} peak field. Variation of susceptibility with temperature was monitored with the MFK1 equipped with a CS3 furnace and a CSL cryostat. Anisotropy of magnetic susceptibility (AMS) was characterized by the shape parameter T (Jelinek, 1981), varying from −1 (prolate) to +1 (oblate), and the anisotropy degree P (ratio of maximum to minimum susceptibility). High field susceptibility (χ_{hf}) was determined by linear fitting of the 0.9–1 T field interval of the hysteresis loops.

Anhysteretic remanent magnetization (ARM) was imparted using the in-line system of the 2G magnetometer. Anisotropy of ARM was measured using a three position scheme (Gattacceca and Rochette, 2002) and was characterized like AMS using P_{rem} (anisotropy degree of remanence) and T_{rem} (shape parameter for remanence). Piezo-remanent magnetization (PRM), used as an analogue for shock remanent magnetization, was imparted through hydrostatic loading and unloading in the presence of a controlled magnetic field using a non-magnetic pressure cell up to 2 GPa (Gattacceca et al., 2010). Partial thermoremanent magnetizations (partial TRM) were acquired using the MMTD furnace. The rates of acquisition and decay of viscous magnetization of the samples were estimated experimentally. The acquisition rate was monitored over a period of two weeks by periodic measurements of the VRM acquired in the terrestrial field. The decay rate was then measured by periodic measurements with the sample kept in a sub-null (∼50 nT) ambient field. VRM acquisition and decay were best fitted using a linear fit with log time with correlation coefficient $R^2 > 0.95$ (Fig. 1). Both rates were found to be approximately the same (Supplemental Table B and Fig. 1) as classically observed (Enkin and Dunlop, 1988).

All magnetic measurements were performed at CEREGE (Aix-en-Provence, France), with the exception of MPMS measurements (at IPGP, Paris, France).

3. Rock magnetism

3.1. Low temperature measurements

Low temperature remanence measurements performed on the Paris and Murchison meteorites show the presence of a Verwey transition around 120 K (Supplemental Fig. A), as previously observed by Elmaleh et al. (2012). Monitoring of magnetic susceptibility of Cold Bokkeveld, Mighei, Nogoya, and Paris at low temperature confirm the existence of a Verwey transition in all samples but one (the less aqueously altered lithology of Paris meteorite, Supplemental Fig. B). The Verwey transition indicates the presence of stoichiometric magnetite with variable abundance at the scale of the measured samples (sample masses 30 to 150 mg). A weak transition around 40 K, is tentatively identified in Murchison (Supplemental Fig. A) which could correspond to the phase transition of monoclinic pyrrhotite at 34 K (Rochette et al., 1990).

3.2. Magnetic susceptibility

For simplicity, magnetic susceptibility (χ) is expressed in log units ($\log\chi$, with χ in 10^{-9} m^3 kg^{-1}, Table 1). Log χ ranges from 3.36 in Mighei to 4.28 in Paris. Our results are in general agreement with values obtained by Rochette et al. (2008) on larger masses of several grams except for Murray which has $\log\chi = 4.22$, much higher than the average value of $\log\chi = 3.82 \pm 0.22$ measured on 7 samples by Rochette et al. (2008). Our Murray sample may be an unusual magnetite-rich clast (Metzler et al., 1992; Rubin and Wasson, 1986), but because the 13 g parent sample has the same susceptibility anomaly ($\log\chi = 4.27$) it is rather a mislabeled or misidentified sample (although it is clearly a CM chondrite). Paramagnetic susceptibility contributes only from 2 to 14% to the total susceptibility in all CM chondrites studied here.

High temperature measurements of magnetic susceptibility for four CM chondrites (Supplemental Fig. B, b) show a Curie temperature at ∼580 °C, corresponding to stoichiometric magnetite. In all samples, a faint downward inflection around 225 °C is observed which may be attributed to the Curie temperature of schreibersite.

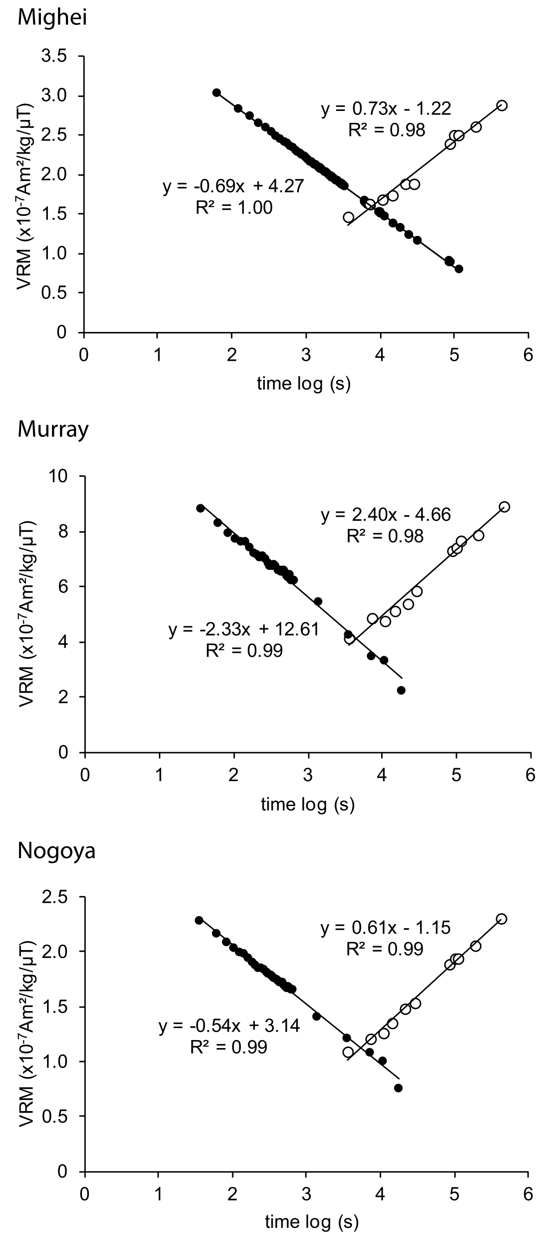

Fig. 1. VRM acquisition in the 47 μT terrestrial field (open symbols) followed by a subsequent decay (filled symbols) for Mighei, Murray and Nogoya chondrites. A linear fit was computed for both experiments. The corresponding equations and coefficient of determination (R^2) are indicated.

For the range of compositions observed in CM chondrites, with Fe/Ni atomic ratio between 0.41 and 4.44 (Nazarov et al., 2009), the expected Curie temperature of schreibersite is between −110 and 300 °C (Gambino et al., 1967). However, schreibersite is found in very small amounts in the studied CM chondrites, with a volume content in the 0 to 14 ppm range and an average of 5 ppm (Nazarov et al., 2009). Its contribution should be below the detection limit of the susceptometer used for this experiment. We therefore have no satisfactory explanation for this inflection at 225 °C. For Paris, we observed two major differences from other CM chondrites: a small inflection around 450 °C and a residual magnetic susceptibility above 585 °C. The second feature is due to metallic FeNi, known from petrographic observations to be abundant in this meteorite (3 vol%). The inflection at 450 °C may be attributed to schreibersite with a composition close to Fe_3P. Schreibersite has been observed in Paris, but not analyzed (Hewins et al., 2014).

Table 1
Petrographic and average intrinsic magnetic properties of studied CM chondrites. Exposure age (Nishiizumi et al., 1993), M_{rs} saturation remanence (acquired in 3 T field), M_s: saturation magnetization, B_{cr}: coercivity of remanence, B_c: coercivity, χ: low field magnetic susceptibility, SD: standard deviation of low field magnetic susceptibility, χ_p: paramagnetic susceptibility. All susceptibilities are in 10^{-9} $m^3\,kg^{-1}$, P_{asm}, T_{asm}: anisotropy degree and shape parameter for magnetic susceptibility, P_f: anisotropy degree of ferromagnetic susceptibility. P_{rem}, T_{rem}: anisotropy degree and shape parameter of anhysteretic remanence, S-ratio (computed as $IRM_{0.3T}$/SIRM). Parameters that were not measured or not available are indicated by –. Results for individual samples are given in details in Supplemental Table A.

Sample	Mass (g)	Exposure age	M_{rs} ($mA\,m^2\,kg^{-1}$)	M_s ($A\,m^2\,kg^{-1}$)	B_{cr} (mT)	B_c (mT)	log χ	SD	log χ_p	P_{asm}	P_f	T_{asm}	P_{rem}	T_{rem}	S ratio (%)
Banten	0.043	2.62	102.3	2.15	89	10	4.03	0.04	2.81	1.10	1.11	0.08	1.10	0.15	–
Cold Bokkeveld	0.028	0.28	60.8	1.53	52	10	3.67	0.31	2.91	1.09	1.10	0.26	1.20	0.58	82.7
Mighei	0.249	1.83	35.8	0.71	58	19	3.36	0.02	2.40	1.05	1.05	0.70	1.13	0.78	90.4
Murchison	0.765	1.34	88.6	0.52	61	23	3.51	–	2.53		–	–	–	–	88.4
Murray	0.273	2.70	117.2	5.69	76	6	4.22	0.16	3.01	1.08	1.08	−0.16	1.10	0.44	80.6
Nogoya	0.520	0.21	87.4	1.05	83	18	3.60	0.16	2.45	1.10	1.10	0.41	1.22	0.71	93.0
Paris	1.839	–	124.0	4.60	66	7	4.28	0.21	2.71	1.12	1.13	0.48	–	–	∼ 83

Table 2
Artificial remanent magnetizations with the corresponding median destructive field (MDF) of the studied CM chondrites. $M_{rs:}$ saturation remanence (SIRM, acquired in 3 T field), ARM: anhysteretic remanent magnetization was acquired in an AF of 100 mT (∗), of 160 mT (+) and a 100 μT steady field. PRM: piezo-remanent magnetization was acquired in 2 GPa in a field of 751.4 μT.

Sample	Mass (g)	M_{rs} ($mA\,m^2\,kg^{-1}$)	MDF of SIRM (mT)	ARM ($mA\,m^2\,kg^{-1}$)		MDF of ARM (mT)	PRM @2 GPa ($mA\,m^2\,kg^{-1}$)	MDF of PRM (mT)
Banten	0.043	102.3	70	0.76	∗	38	–	–
Cold Bokkeveld	0.028	60.8	37	0.42	∗	29	0.49	11
Nogoya	0.520	87.4	61	0.39	∗	29	0.39	14
Mighei	0.249	35.8	40	0.29	∗	34	0.14	16
Murray	0.273	117.2	59	0.94	∗	31	1.08	3
Murchison	0.765	88.6	38	0.87	+	56	0.41	15
Paris	1.839	124.0	47	1.43	+	45	0.84	11

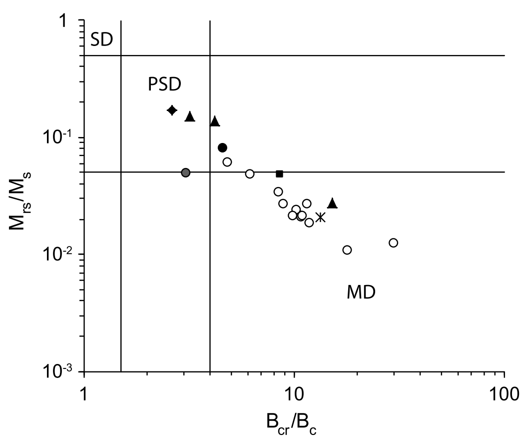

Fig. 2. M_{rs}/M_s versus B_{cr}/B_c for seven CM chondrites studied in this work. Banten (box), Cold Bokkeveld (triangles), Mighei (gray circle), Murchison (diamond), Murray (star), Nogoya (solid circle), Paris (open circles). The limits for the single domain (SD), pseudo single domain (PSD), and, multi-domain (MD) are indicated (Day et al., 1977).

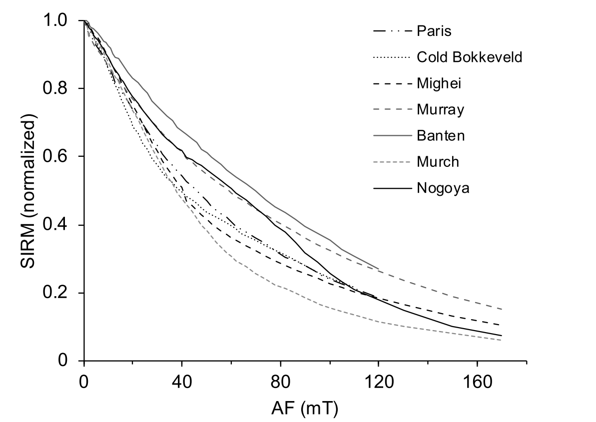

Fig. 3. Normalized intensity of SIRM (acquired in a field of 3 T) versus AF for the studied CM chondrites.

3.3. Hysteresis properties

Hysteresis properties show large variability among the studied CM chondrites, indicating variable magnetic mineral assemblages and abundances (Table 1, Supplemental Fig. C). M_s varies between 0.52 $A\,m^2\,kg^{-1}$ (Murchison) and 5.69 $A\,m^2\,kg^{-1}$ (Murray). M_{rs} varies between 3.58×10^{-2} (Mighei) and 1.24×10^{-1} $A\,m^2\,kg^{-1}$ (Paris). The S ratio varies between −0.83 (Mighei) and −0.93 (Nogoya) (Table 1), indicating the significant presence of a high coercivity mineral, likely sulfides. The curved shape of hysteresis cycles up to 1 T suggests a noticeable contribution of metallic iron (or possibly schreibersite) except in Cold Bokkeveld (Supplemental Fig. C). The hysteresis parameters indicate an overall multidomain (MD) to pseudo-single domain (PSD) behavior with a mean M_{rs}/M_s of 6.2×10^{-2} (Fig. 2), but because the magnetic mineralogy is a mixture of magnetite, sulfides, and metal, this apparent domain state is not relevant for the interpretation of the paleomagnetic data.

The possible link between aqueous alteration degree and magnetic mineralogy is not discussed here as it requires further investigations.

3.4. Remanent magnetization

We have investigated the ARM, PRM, saturation IRM (SIRM) and VRM of all studied samples. Their intensities are reported in Table 2 and Supplemental Table B. PRM intensity increases with pressure up to 2 GPa (Supplemental Fig. D), and the coercivity spectrum is shifted towards higher coercivity values with increasing pressure (Supplemental Table C) as classically observed (e.g., Gattacceca et al., 2010).

The median destructive field (MDF) quantifies the stability of remanence against AF demagnetization (Table 2). MDFs of SIRM range from 37 mT in Cold Bokkeveld to 70 mT in Banten (mean value 50 mT) (Fig. 3). The ARM also exhibits a broad range of stability with MDFs ranging from 29 (Cold Bokkeveld and Nogoya) to 56 mT (Murchison). PRM acquired at 2 GPa shows a lower range of coercivity with MDF in the range 2–15 mT.

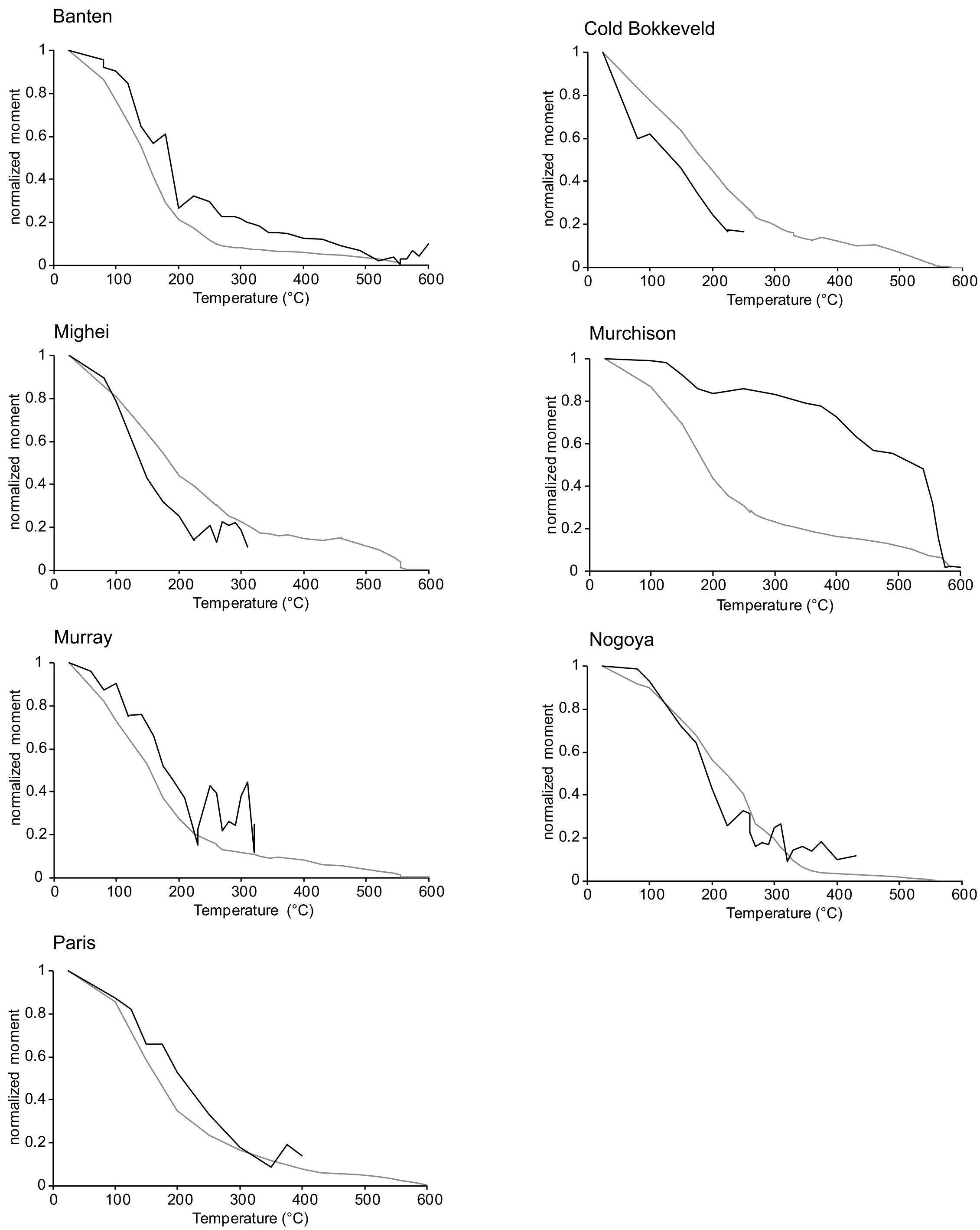

Fig. 4. Normalized intensities of NRM (black line) and SIRM (gray line) versus thermal demagnetization for the studied CM chondrites.

Thermal demagnetization of the SIRM shows variable behavior (Fig. 4). All CM chondrites are demagnetized at relatively low temperature with less than ∼20% of the magnetization remaining at 320 °C. This suggests that sulfides dominate the remanence signal, given that schreibersite is ruled out by its low abundance (see Section 3.3). In Mighei and Nogoya, two inflections are present around 270 and 320 °C, characteristic of hexagonal and monoclinic pyrrhotite, respectively. However, these Curie points are not well expressed in general and the range of unblocking mainly below 200 °C suggests complexity in the magnetic mineralogy, possibly linked with Ni substitution and mineral defects in pyrrhotites. Metallic iron was detected in Murchison and Cold Bokkeveld with an intensity drop around 770 °C during measurements of induced magnetization versus temperature (Banerjee and Hargraves, 1971, 1972). However, our experiments show that this metallic iron does not carry any significant remanence compared to pyrrhotite and magnetite.

VRM acquisition and decay rates allow the computation of the maximum VRM (VRM_{max}) that may have been acquired during the terrestrial residence of the samples (Supplemental Table B). VRM_{max} is computed for the unfavorable case where samples were kept in a fixed position in a terrestrial magnetic field of ∼50 μT since their fall and taking into account the decay of the VRM in the shielded room prior to our NRM measurements. The results show that VRM contributes less than 10% of the measured NRM in Murray and Cold Bokkeveld, in agreement with previous

Table 3
Paleomagnetic interpretation obtained from the studied CM chondrites. Demagnetization treatment used; AF (alternating field) and TH (thermal). NRM = Natural remanent magnetization, Total REM = NRM/SIRM, LC = low coercivity component, HC = high coercivity component, LT = low temperature, HT = high temperature. REM′: REM′ (as defined in Gattacceca and Rochette, 2004) integrated over the given AF stability range (with associated paleofield estimate). For each component defined inclination, declination, maximum angular deviation (MAD) and the number of points used are given (n).

Sample	Treatment	NRM ($mA\,m^2\,kg^{-1}$)	Total REM ($*10^3$)		AF/thermal range (mT or °C)	D	I	MAD	n	REM′ ($*10^3$)	Paleofield (μT)
Banten	AF + TH	0.772		LC/LT	1 mT–80 °C	267.6	−31.8	12.1	5		
				HT	120–460 °C	194.4	−66.7	4.3	16		
Cold Bokkeveld+	AF	2.510	5.59	LC	1–7 mT	88.2	−68.9	5.5	10	20.76	62
				HC	9–110 mT	18	10.7	0.9	40	6.59	20
Cold Bokkeveld	AF	0.062	1.34	LC	6–15 mT	71.4	0.3	4.0	9	2.59	8
	AF	0.216	2.88	LC	6–15 mT	73.4	11.5	2.4	10	6.39	19
	AF	0.078	1.87	LC	7–17 mT	77.5	−2.2	7.1	13	3.83	12
	AF	0.131	1.75	LC	5–22 mT	69.6	−4.1	6.4	17	2.43	7
	AF + TH	0.113		LC	0–10 mT	80.2	4.6	1.8	15		
				HT	100–260 °C	15.6	−36.8	17.6	7		
Mighei	AF	0.016	0.44	LC	0–8 mT	295.8	−41.7	5.4	13	3.67	11
				HC	11–105 mT	192.3	20.6	23.7	26	0.31	1
	AF + TH	0.011		LC	0–5 mT	310.1	−29.2	3.5	9		
				HT	100–290 °C	190.7	27.6	10.6	11		
Murchison	AF	0.034	0.39	LC	1–5 mT	52.3	−30.3	1.9	7	4.87	15
				HC	20–100 mT	193.1	−27.4	11.2	29	0.34	1
	AF + TH	0.284		LC	1–5 mT	353.7	−20.6	4.1	7		
				HT	200–520 °C	186.0	−40.3	12.5	8		
Murray	AF	0.215	1.84	LC	0–4 mT	313.9	−18.4	5.1	9	20.85	63
				HC	4–110 mT	262.6	−51.2	2.1	46	0.79	2
	AF + TH	0.185		LC	0–4.5 mT	304.7	−12.4	3.8	7		
				HT	100–270 °C	252.8	−33.6	17.7	13		
	AF + TH	0.475		LC	1–4 mT	318.6	−34.2	3.3	5		
				HT	100–260 °C	234.0	3.4	11.3	8		
Nogoya	AF	0.025	0.28	LC	0–6 mT	192.3	−23.9	7.5	11	1.84	6
				HC	8–78 mT	310.3	−2	7.1	35	0.19	1
	AF + TH	0.015		LC	0–3.5 mT	195.0	−9.5	13.3	7		
				HT	150–290 °C	284.4	−22	10	9		
Paris-1	AF	0.229	2.44	LC	2–7 mT	26.4	7	7.6	7	7.34	22
				HC	11–58 mT	310.2	75.5	16.4	22	0.63	2
Paris-2	AF	1.600	12.74	LC	1–4 mT	197.8	0.2	2	7	142.08	426
				MC	20–32 mT	51.2	35.6	2.5	7	18.36	55
				HC	44–100 mT	86.8	44.7	9.9	10	1.76	5
Paris-3	AF	1.550	16.44	LC	0–2 mT	182.8	24.4	1.4	4	33.08	99
				MC	11–20 mT	93.7	29.6	2.5	7	55.11	165
				HC	26–110 mT	114.3	80.4	14.2	29	1.32	4
Paris-4	AF	0.880	4.50	LC	2–6 mT	147	28	1.2	7	40.11	120
				HC	14–56 mT	168	78.4	7.8	16	0.58	2
Paris-5	AF	1.360	10.12	LC	2–10 mT	159.5	25.7	2.2	5	53.78	161
				HC	24–90 mT	192	77.2	8.8	21	0.62	2
Paris-6	AF + TH	0.125		LC	2–10 mT	143.7	34.2	11.3	9		
				HT	175–585 °C	15.5	75.3	22.6	16		

For Cold Bokkeveld, sample with fusion crust is indicated by "+".

results (Brecher and Arrhenius, 1974). For Mighei and Nogoya, VRM_{max} amounts to 99 and 61% of the NRM, respectively. In view of the terrestrial residence time of the studied meteorites (50 to ~200 years), the terrestrial VRM is expected to be stable up to 80–120 °C upon laboratory thermal demagnetization, depending on whether it is carried by pyrrhotite or magnetite (Pullaiha et al., 1975; Dunlop et al., 2000).

3.5. Magnetic anisotropy

Characteristic parameters describing the AMS are presented in Table 1. Anisotropy degrees are weak, with P ranging from 1.05 (Mighei) to 1.10 (Nogoya and Banten), and mean value 1.08. The Paris meteorite is the most anisotropic ($P = 1.12$) likely due to its higher content of metallic iron. The shapes of the susceptibility ellipsoids are neutral to oblate. Mutually oriented samples have a similar orientation of the anisotropy axes (Supplemental Fig. E), indicating a homogeneous fabric at the scale of about 1 cm (initial size of the largest studied samples). The anisotropy of ARM is also weak (P_{rem} ranges from 1.10 to 1.22) and oblate. The principal axes of susceptibility and ARM ellipsoids have similar directions. The observed homogeneity of the fabric in our CM samples suggests that our samples are smaller than the clasts size, or that fabric was imparted by post-brecciation shock compaction (see e.g., Gattacceca et al., 2005).

4. Paleomagnetic results

AF demagnetization up to 170 mT was performed on at least one subsample of each studied meteorite. Thermal demagnetization was also conducted after removal of the low coercivity (LC) component with AF demagnetization. The directions of the components were computed using principal component analysis (Kirschvink, 1980). The results are listed in Table 3, and displayed in Figs. 5, 6 and 7.

For Cold Bokkeveld, one sample with fusion crust and four interior mutually-oriented samples were demagnetized with AF. NRM intensity averages $1.2 \pm 0.4 \times 10^{-4}$ $Am^2\,kg^{-1}$ in the four interior

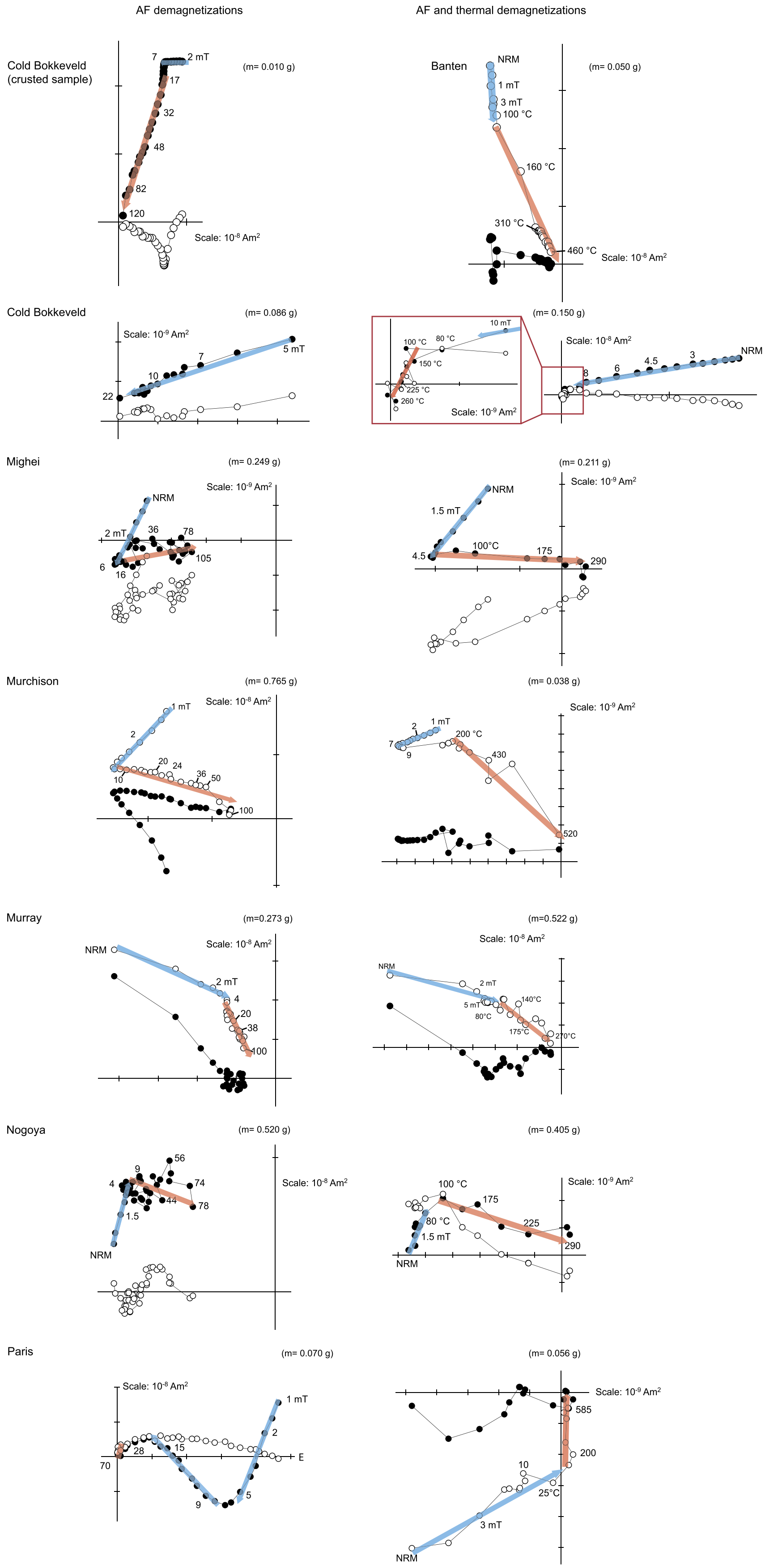

Fig. 5. Orthogonal projections of AF and thermal demagnetization data for the studied CM chondrites. Low coercivity (LC) (and medium coercivity (MC) for Paris) components of magnetization are indicated by a blue arrow. High coercivity (HC) and high temperature (HT) components of magnetization interpreted as a possible primary CRM (see text) are indicated by a red arrow. (For interpretation of the references to color in this figure legend, the reader is referred to the web version of this article.)

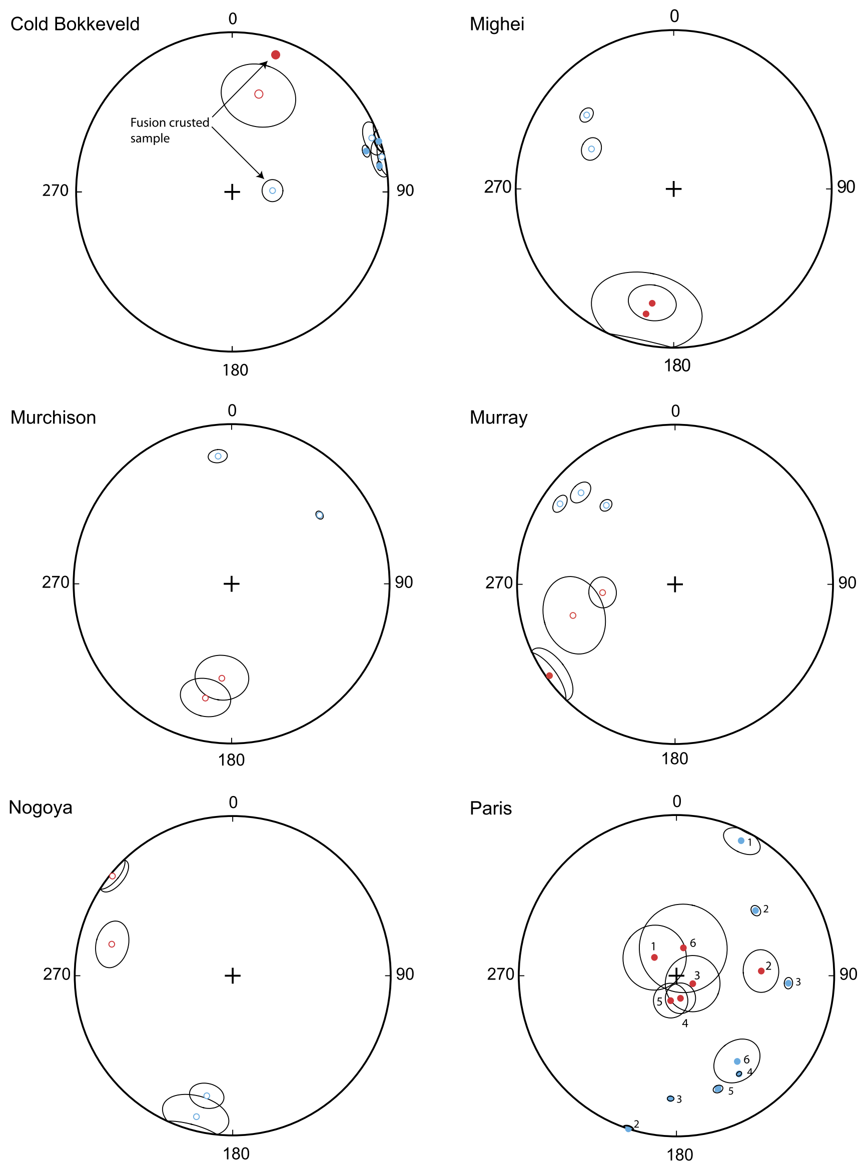

Fig. 6. Stereographic projection of the stable component of magnetization (and their 95% confidence interval) for the CM chondrites where multiple mutually-oriented samples were studied. Open and solid symbols are projection in the upper and low hemisphere respectively. Blue symbols represent LC (and MC for Paris) components and red symbols represent HC/HT components (ChRM). For Paris each sample is identified by a specific number. (For interpretation of the references to color in this figure legend, the reader is referred to the web version of this article.)

samples and reaches 2.5×10^{-3} $Am^2\,kg^{-1}$ for the sample with fusion crust. The fusion crusted sample possesses two stable components of magnetization (Fig. 5): a low coercivity component (1–7 mT) and a high coercivity (HC) component interpreted as a TRM acquired in the Earth's field during atmospheric entry. In all four interior samples, the demagnetization data reveal a single LC component almost trending towards the origin and fully demagnetized by 20 mT (Fig. 5). The erratic behavior observed above 20 mT is in agreement with previous measurements showing that the NRM of Cold Bokkeveld is essentially demagnetized by 30 mT (Brecher and Arrhenius, 1974). All LC components have essentially identical direction in all sub-samples, but differ from both directions found in the fusion crust (Fig. 6). One sample was thermally demagnetized (following removal of the LC component by AF demagnetization up to 10 mT), and shows a faint origin-trending HT component between 100 and 260 °C (Fig. 5). This HT component accounts only for ∼10% of the total magnetization.

For Mighei, two mutually-oriented samples were studied, one with AF demagnetization and one with thermal demagnetization. AF demagnetization reveals an LC component (0–8 mT) and a well-defined HC component (11–105 mT) (Fig. 5). After removal of the LC component by AF, thermal demagnetization reveals a stable component between 100 and 290 °C (Fig. 5). Above 290 °C, demagnetization is chaotic probably because of the occurrence of thermal alteration during demagnetization process. The direction isolated by thermal demagnetization is similar to the HC direction and is essentially origin-trending, although a weaker high temperature component may exist (Fig. 6).

For Murchison, two mutually-oriented samples were studied. The HC and HT components, isolated up to 100 mT and 520 °C, respectively, by AF and thermal demagnetization (Fig. 5), have similar directions and trend towards the origin (Fig. 6).

For Murray, three mutually-oriented samples were studied. The NRM intensities are homogeneous. AF demagnetization of one sample reveals an LC component between 0 and 4 mT. Between 4 and 110 mT, an HC component is partially demagnetized (Fig. 5). The HC direction was computed by anchoring demagnetization data to the origin. AF demagnetization of the two other samples up

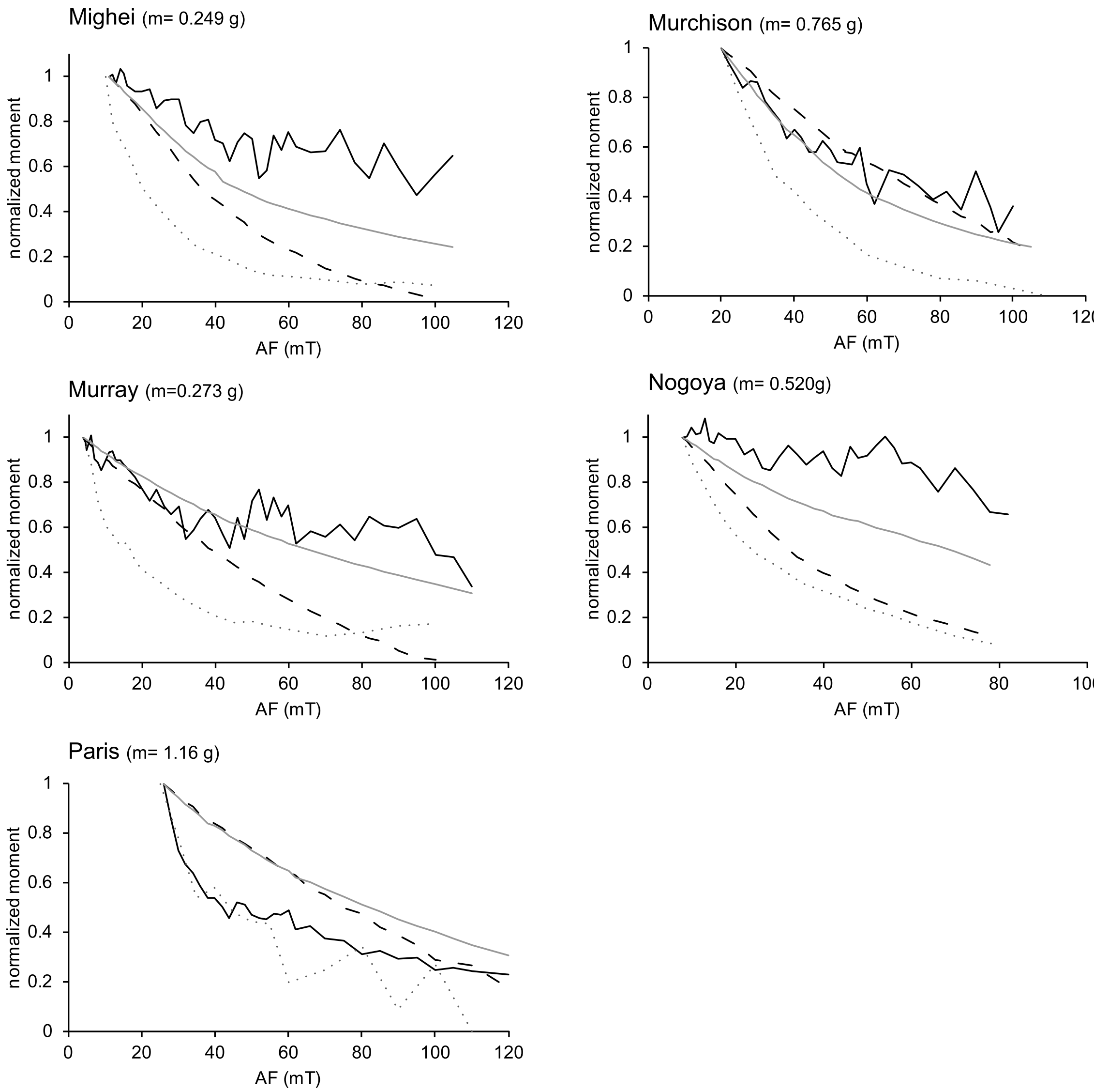

Fig. 7. Normalized intensities of ChRM (full black line), ARM (black dashed line), IRM (full gray line) and PRM (gray dotted line) versus alternating field for the CM chondrites demagnetized with AF.

to ∼6 mT reveals a similar LC component. In these samples, a stable HT component is isolated above 100 °C and up to 270 °C and 260 °C, respectively. Above these temperatures, demagnetization is chaotic likely because of alteration during demagnetization process. The HC and HT components have similar directions (Fig. 6).

For Nogoya, two mutually-oriented samples were studied. After removal of an LC component below ∼5 mT, a stable HC component was partially demagnetized up to 78 mT (Fig. 5), followed by erratic behavior for higher fields. As for Murray, the direction of the HC component was computed by anchoring to the origin. Thermal demagnetization reveals a stable component between 150 and 290 °C (Fig. 5). Above 290 °C demagnetization is chaotic likely because of alteration during demagnetization process. HC and HT components directions are comparable (Fig. 6). Both of these components are essentially origin-trending although a smaller higher temperature component may exist.

For Banten, a single sample was investigated through thermal demagnetization. It reveals a low temperature component isolated below 80 °C and an origin-trending HT component between 120 and 460 °C (Fig. 5). At higher temperature, demagnetization behavior becomes unstable probably due to sample alteration that occurred with heating.

For Paris six mutually-oriented samples were studied. One sample was thermally demagnetized and five samples were AF demagnetized. All samples show one or two LC components blocked below ∼12 mT, and an HC component isolated above ∼25 mT and up to 85 mT (Fig. 5). The LC components lie on a great circle whereas the HC components are clustered (Fig. 6). Thermal demagnetization of a sample previously demagnetized by AF up to 10 mT also reveals two components of magnetization: an LC and low temperature (LT) component, isolated up to 80 °C and lying on the same great circle as the LC components, and a high temperature (HT) component isolated between 175 and 585 °C (Fig. 5) that has a similar direction to the HC components (Fig. 6). Most demagnetization trends have a curved shape and high ratios of NRM to SIRM above 0.05 up to AF demagnetization at 20 mT (Table 3), indicative of contamination by a strong field typical of artificial magnets.

5. Discussion

5.1. Nature of the NRM

We identified two stable components of magnetization in all studied CM chondrites. These two components were best isolated by thermal demagnetization. An LC component was usually isolated below ∼15 mT and an HC component between ∼20 and ∼90 mT. A HT component was isolated between ∼120 °C and 260 to 585 °C. The HC and HT directions isolated by AF and thermal demagnetization, respectively, in mutually-oriented samples are similar considering their 95% confidence interval and the sub-samples orientation precision (Fig. 6). These directions are called characteristic remanent magnetization (ChRM) in the following discussion. The ChRM trend essentially towards the origin, although is some cases a weak higher temperature component may exist, with an intensity of less than 10% of the ChRM intensity. Overall, our results agree with previous studies that found the presence of at least a one well-preserved stable remanence component in Cold Bokkeveld, Mighei, Murray and Murchison meteorites through AF demagnetization up to 30 mT (Larson et al., 1973; Brecher and Arrhenius, 1974; Kletetschka et al., 2003).

Except for Paris that has been contaminated with a strong field (magnet) and Cold Bokkeveld (discussed below), the LC components, whose intensities are on the order of, or lower than, the HC/HT components are likely of viscous origin or the result of magnetic contamination during sample curation, handling, and/or preparation. These terrestrial components are not discussed in further details. In Cold Bokkeveld, the LC component extends to higher AF than in the other studied CM chondrites, and its intensity is ten times that of the HC/HT component, VRM cannot account for more than about 10% of the LC/LT component. Partial TRM experiments show that the LC/LT component scales well with a partial TRM acquired at 100 °C in a field of ∼50 μT, similar to the Earth field. Therefore the LC/LT component could have been acquired through moderate heating during atmospheric entry. This LC/LT direction show a 90° difference with the directions determined for the fusion crust, but this can be accounted for by the time lag for the diffusion of the thermal wave associated with atmospheric entry (e.g., Sears, 1975) and the fact that the meteorite may be rotating in the atmosphere (e.g., Adolfsson and Gustafson, 1994).

The determination of the nature of the ChRM is crucial for estimating and interpreting the paleofield intensity. CM chondrites are brecciated meteorites that have been aqueously altered at low temperatures (<40 °C, see Section 1.1) and shocked to relatively low pressures (<5 GPa). As such, a number of mechanisms might account for their NRM.

The main magnetic minerals in CM chondrites are magnetite and pyrrhotite. A minor fraction of the pyrrhotite is primary (cf. Section 1.2), whereas magnetite and a large fraction of pyrrhotite were produced by aqueous alteration (Hyman and Rowe, 1983; Zolensky and McSween, 1988; Brearley and Jones, 1998; Bullock et al., 2010). Because these magnetic minerals are secondary and because the ChRM is homogeneous in direction at least at the cm scale, a pre-accretional magnetization acquired when the materials were free-floating in the protoplanetary disk is ruled out.

Primary pyrrhotite, formed in chondrules before accretion, cannot account significantly for the measured ChRM. Indeed, whether it was magnetized or not before accretion, the accretion process will result in a null magnetization as the sum of a large number of randomly oriented chondrule magnetizations. Moreover the primary pyrrhotite fraction is minor compared to the secondary one, and it is much coarser (see Section 1.2) making it a less efficient magnetic recorder.

The secondary nature of the magnetic minerals carrying the NRM also rules out acquisition of detrital NRM during accretion on the parent body, a possibility proposed by Fu and Weiss (2012). Because the studied meteorites have never been subjected to temperatures above ∼40 °C (Cody et al., 2008; Kimura et al., 2011), the ChRM (unblocked up to ∼300 °C or higher) cannot be a TRM or a partial TRM. Moreover, if it was a TRM, the ChRM would have a similar demagnetization behavior as ARM, which is not observed except for Murchison and Murray (Fig. 7).

This leaves the following post-accretional mechanisms: CRM by crystallization of magnetite and pyrrhotite during aqueous alteration, shock magnetization during impacts suffered by the parent asteroid, thermal magnetization acquired in the Earth field during atmospheric entry or VRM in the Earth field.

Comparison of the intensity of the ChRM with the maximum VRM estimates (Supplemental Table B) show that VRM cannot account for the ChRM except for Mighei and Nogoya. Moreover, the ChRM is unblocked up to ∼300 °C or above, which is notably higher than the expected stability temperature range for a terrestrial VRM (80–120 °C, see Section 3.4).

To further assess the nature of the ChRM we compared the AF demagnetization behavior of ChRM, ARM [an analogue for TRM (Stephenson and Collinson, 1974)], SIRM and PRM (an analogue for shock remanent magnetization) over the AF interval used to define the HC component for each CM chondrite (Fig. 7).

The behavior of PRM (acquired at 2 GPa) is different from that of ChRM in all studied CM chondrites, except for Paris. Moreover, if the ChRM was a PRM, it would require a minimum ambient field in the range 42–760 μT at the time of impact (635 μT for Paris). This field is computed by extrapolating our PRM experiments to 5 GPa using an exponential fit, the maximum shock pressure potentially suffered by these meteorites (Supplemental Fig. D). This paleointensity may be too high regarding magnetic fields intensities which prevailed in the early solar system history to be realistic (maximum 100 μT in the midplane of the disk, e.g., Turner and Sano, 2008, and see Section 5.3). Therefore, the ChRM cannot be a shock remanent magnetization.

Therefore, the only possibility is that the ChRM of Mighei, Murray, Murchison, Nogoya and Paris are CRMs, as already suggested by Banerjee and Hargraves (1971) and Larson et al. (1973). For Banten (which was not studied with AF) and Cold Bokkeveld (for which the ChRM is isolated only through thermal demagnetization) comparison of AF demagnetization behavior of ChRM with artificial remanence is not available, but we think that the CRM interpretation can be safely extended to these two meteorites. This interpretation is in good agreement with the similar thermal demagnetization of ChRM and IRM in these meteorites (Fig. 4). Indeed, in view of the absence of thermal events, the correlation between the ChRM unblocking temperatures and the magnetic mineralogy is a strong indication that the ChRM is the product of crystallization of the magnetic carriers in the presence of a magnetic field. In all studied samples, the unblocking temperatures around 220 °C indicate that the ChRM is mostly carried by sulfide (pyrrhotite). The dominance of pyrrhotite is also suggested by the better results achieved with thermal demagnetization than with AF demagnetization. Murchison is an exception with the ChRM mostly carried by magnetite as shown by major NRM unblocking temperatures around 570 °C and the good results achieved through AF demagnetization.

It can be estimated from the time-temperature stability diagrams for magnetite and pyrrhotite (Pullaiah et al., 1975; Dunlop et al., 2000) that a rock magnetized at 4.5 Gyr and subsequently kept in null magnetic field in the asteroid belt at an average temperature of about −110 °C (e.g., Spencer et al., 1989) will be viscously erased only to ∼20 or 60 °C whether it is carried by pyrrhotite or magnetite, respectively. The transfer time from the asteroid belt to the Earth in the form of a meteoroid is spent mostly in the vicinity of the asteroid belt (Gladman et al., 1997). Therefore no significant amount of time is spent in a near-Earth orbit that would result in further viscous decay of the original remanent magnetization. In view of the relatively short cosmic ray exposure (CRE) age of some CM chondrites (Table 1), it has been hypothesized that the CMs may originate from near Earth objects

(NEOs) (Morbidelli et al., 2006). The typical dynamical lifetime of NEOs is limited to a few Myr (Farinella et al., 1994). A one Myr stay as a NEO, with equilibrium temperature around 0 °C, would unblock the remanence up to only 80 °C for pyrrhotite and 150 °C for magnetite. Because the ChRMs measured in CM chondrites are mostly carried by pyrrhotite and unblocked above 100 °C, they would be unaffected even if CM chondrites originate from NEOs. This is also true for Murchison that has its ChRM carried mostly by magnetite and unblocked above 200 °C. Moreover organic matter in CM chondrites would degrade very fast during exposure to temperatures found in the vicinity of the Earth's orbit, for example in less than 1000 years at 0 °C for Murchison (Kebukawa et al., 2010). This is another indication that the CM chondrites did not experience temperatures of the order of 0 °C for any period of time that would lead to significant viscous magnetization.

It is noteworthy that all CM chondrites are brecciated at the cm scale (see Section 1.2). This needs to be reconciled with the observed homogeneity of ChRM directions in our samples. Either ChRM was acquired after brecciation (i.e. aqueous alteration postdated brecciation), which may be at odd with the juxtaposition in some CM chondrites of clasts with variable degrees of aqueous alteration, or our samples are small compared to the brecciation scale. We favor the second possibility, all the more because the magnetic fabric is also homogeneous within our samples (see Section 3.5). In both cases, the paleomagnetic record of our samples is likely not disturbed by the brecciation process.

5.2. Paleointensities

There is no technique for retrieving precise paleointensities from a CRM. We used the REM' normalization technique that is calibrated for TRM (Gattacceca and Rochette, 2004; Wasilewski et al., 2002) for all samples except Banten which was not studied with AF. However, CRM can be less efficient than TRM (McClelland, 1996) so the estimated paleointensity should be regarded as a lower limit. This is all the more true that this normalization technique takes into account the primary pyrrhotite that does not contribute to the ChRM. Although primary pyrrhotite represents a minor fraction of the total pyrrhotite, this leads to additional slight underestimation of paleointensities. The minimum paleointensities derived from the HC component for Paris, Mighei, Nogoya, Murchison and Murray are in the range 1 to 5 μT (Table 3). For Cold Bokkeveld, for which the HC component cannot be resolved by AF demagnetization, we estimate the paleofield using the residual REM at 20 mT (ratio of NRM and IRM after demagnetization at 20 mT). This residual REM averages 5×10^{-4}, indicating a paleofield of ∼1.5 μT. This value falls in the range defined for other CM chondrites. Therefore, the mean minimum paleointensity defined for all samples is 2.1 ± 1.5 μT (Table 3). For Murchison our minimum paleointensity estimate of ∼1 μT is in broad agreement with a previous estimate in the 0.2 to 2 μT range (Kletetschka et al., 2003).

5.3. Magnetizing field

The CRM nature of the magnetization implies that the magnetizing field must have been stable (with respect to the asteroid) during aqueous alteration that took place between roughly 2.4 and 4 Myr after CAI formation, either as a single event or episodically (see Section 1.1).

Two alternatives exist to account for a non-transient magnetic field of ∼2 μT in the early solar system: an external magnetic field (in the protoplanetary disk) or an internal field generated within the parent body by some form of dynamo process. The paleointensity and the age of the magnetization mentioned above might help discriminating between the two possibilities.

Theoretical analyses indicate that early planetesimals were likely capable of generating core-dynamos soon after the formation of the solar system. Hf/W chronometry suggests core formation at 3.8 ± 1.3 Myr after CAI formation for asteroid Vesta (Kleine et al., 2002) and at 1 to 1.5 Myr after CAIs for many planetesimals (Kruijer et al., 2012). Dynamo scaling laws suggest that small body dynamos could produce core magnetic fields that fall in the of range 0.1–150 μT (Weiss et al., 2010; Tarduno et al., 2012). The surface field intensities estimated in this study are therefore in the range expected for planetesimal core dynamos. Therefore, it is possible that the CM chondrite parent body had a dynamo field in its early history. This hypothesis implies the presence of a highly conductive liquid core. We may also consider alternatives to the liquid metal core hypothesis, based on the abundance of liquid water in the CM parent body. Liquid water may reach high electrical conductivity in case of ionic state. However, this requires unrealistically high pressure and temperature, i.e. reached below 2000 km depth in Uranus (Redmer et al., 2011). Magnetic field generation in hydrothermal cells on Earth has been proposed, based on the electrokinetic effect (Zlotnicki and le Mouel, 1990; Adler et al., 1999). However, the corresponding fields are of the order of 10 nT only and are transient. Therefore a dynamo on the CM parent body would likely require a metallic liquid core, i.e. partial differentiation with a molten interior and relic chondritic crust. This has been already proposed for the CV chondrite parent body (Carporzen et al., 2011; Elkins-Tanton et al., 2011; Weiss and Elkins-Tanton, 2013). Recently Fu and Elkins-Tanton (2014) have shown that in a CM-like parent body, the buoyancy of silicic magma generated by internal melting is such that it will preserve an undisturbed crust of pristine chondritic material. Dynamo fields have been identified on a number of relatively small bodies: the angrite parent body from 4564 to at least 4558 Ma (Weiss et al., 2008), the CV parent body at ∼4559–4560 Ma (Carporzen et al., 2011), the pallasite parent body (Tarduno et al., 2012) and asteroid Vesta (Fu et al., 2012).

On the other hand, a field of external origin (or at least some of its components) would have to be stable with respect to the parent body over timescales long enough to allow CRM acquisition. It is generally believed that most carbonaceous chondrites were formed at 3.5 AU (in the asteroid belt region) or farther from the protosun (Clayton et al., 1976, 1977). At this distance, even the most active T-Tauri Sun would result in fields of just 0.001–0.01 μT (Weiss and Elkins-Tanton, 2013). Magnetohydrodynamical simulations predict that fields of the order of 1–100 μT can be generated in the midplane at this location, but these fields may periodically reverse every few hundred years (Gammie, 1996; Turner and Sano, 2008; Bai and Stone, 2013). A more likely external magnetic field source for CM magnetization is the stable, vertical (out-of-the-disk plane) ∼10 μT field expected to be inherited from the parent molecular cloud during gravitational collapse (Crutcher, 2012).

Comparing the estimated duration of aqueous alteration with the timescales of the different magnetic fields does not allow us to discriminate between an internal or external magnetic field origin to account for the magnetization of the CM chondrites.

6. Conclusion

We performed magnetic measurements on seven CM chondrites. The magnetic mineralogy of all studied meteorites is composed of variable amounts of pyrrhotite and magnetite formed during aqueous alteration on the parent body, as well as primary pyrrhotite and metallic FeNi. Although magnetite dominates the magnetic susceptibility of all studied CM chondrites, pyrrhotite dominates the remanent properties of all of them with the exception of Murchison (dominated by magnetite). Paris is the sample containing the most significant fraction of metallic FeNi.

The studied CM chondrites possess one high coercivity and high temperature component of NRM. This component is homogeneous in direction and intensity at the scale of our samples (cm). We interpret this component as a pre-terrestrial CRM acquired during crystallization of magnetite and pyrrhotite on the parent asteroid during aqueous alteration in a field of at least a few μT (minimum estimate 2 ± 1.5 μT).

Magnetite and pyrrhotite were formed by a single or episodic aqueous alteration events over a period encompassing at least 2.4–4 million years after CAIs formation. During this time interval, both internally generated fields (from a putative dynamo) and external fields of nebular origin may have existed. It is impossible so far to discriminate between the two hypotheses. Whatever the nature of the magnetizing field, CM chondrites, relics from the early solar system, likely contain the oldest paleomagnetic record identified to date.

Acknowledgements

We acknowledge France Lagroix (IPGP) for MPMS measurements and François Demory (CEREGE) for assistance in the laboratory. Funding from ANR (project ANR-09-BLAN-0042), and Marie Curie People Programme (FP7/2077-2013, REA grant agreement No. 29835) are acknowledged. We thank the anonymous reviewer and the Professor Adrian Brearley for their constructive review.

Appendix A. Supplementary material

Supplementary material related to this article can be found online at http://dx.doi.org/10.1016/j.epsl.2014.11.019.

References

Adler, P.M., Le Mouel, J.L., Zlotnicki, J., 1999. Electrokinetic and magnetic fields generated by flow through a fractured zone: a sensitivity study for La Fournaise volcano. Geophys. Res. Lett. 26, 795–798.

Adolfsson, L.G., Gustafson, A.S., 1994. Effect of meteoroid rotation on atmospheric entry heating and meteor beginning height. Planet. Space Sci. 42, 593–598.

Aléon, J., Engrand, C., Leshin, L.A., McKeegan, K.D., 2009. Oxygen isotopic composition of chondritic interplanetary dust particles: a genetic link between carbonaceous chondrites and comets. Geochim. Cosmochim. Acta 73, 4558–4575.

Alexander, C.M.O.d., Cody, G.D., Bowden, R., Fogel, M.L., Herd, C.D.K., 2010. Parent body modification of the structure, and elemental and isotopic compositions of IOM in Tagish Lake. Meteorit. Planet. Sci. Suppl. 73, 5367.

Anders, E., 1971. Meteorites and the early solar system. Annu. Rev. Astron. Astrophys. 9, 1–34.

Bai, X.-N., Stone, J.M., 2013. Wind-driven accretion in protoplanetary disks – I: suppression of the magnetorotational instability and lauching of the magnetocentrifugal wind. Astrophys. J. 769. arXiv:1301.0318.

Banerjee, S.K., Hargraves, R.B., 1971. Natural remanent magnetization of carbonaceous chondrites. Earth Planet. Sci. Lett. 10, 392–396.

Banerjee, S.K., Hargraves, R.B., 1972. Natural remanent magnetization of carbonaceous chondrites and the magnetic field in the early solar system. Earth Planet. Sci. Lett. 17, 110–119.

Bischoff, A., 1998. Aqueous alteration of carbonaceous chondrites: evidence for preaccretionary alteration – a review. Meteorit. Planet. Sci. 33, 1113–1122.

Brearley, A.J., 2003. Nebular versus parent-body processing. In: Davis, A.M. (Ed.), Meteorites, Comets, and Planets. In: Treatise on Geochemistry, vol. 1. Elsevier, Oxford, pp. 247–268.

Brearley, A.J., 2006. The action of water. In: Lauretta, D., McSween Jr., H.Y. (Eds.), Meteorites and the Early Solar System II". Arizona University Press, pp. 587–624.

Brearley, A.J., 2011. Alteration of coarse-grained Fe and Fe, Ni sulfides in the Mighei CM2 carbonaceous chondrite: evidence for the instability of primary pyrrhotite–pentlandite grains during aqueous alteration. Lunar Planet. Sci. 42. abstract#2233.

Brearley, A.J., Jones, R.H., 1998. Chondritic meteorites. Rev. Miner. 36, 313–398.

Brearley, A.J., Martinez, C., 2010. Ubiquitous exsolution of pentlandite and troilite in pyrrhotite from the TIL91722 CM2 carbonaceous chondrite: a record of low temperature solid state process. Lunar Planet. Sci. 41. Abstract#1689.

Brecher, A., Arrhenius, G., 1974. The paleomagnetic record in carbonaceous chondrites: natural remanence and magnetic properties. J. Geophys. Res. 79 (14), 2081–2106.

Browning, L., McSween, H., Zolensky, M., 1996. Correlated alteration effects in CM carbonaceous chondrites. Geochim. Cosmochim. Acta 60, 2621–2633.

Bullock, E.S., McKeegan, K.D., Gounelle, M., Grady, M.M., Russell, S.S., 2010. Sulphur isotopic composition of Fe–Ni sulphide grains in CI and CM carbonaceous chondrites. Meteorit. Planet. Sci. 45, 885–898.

Burgess, R., Wright, I.P., Pillinger, C.T., 1991. Determination of sulfur-bearing components in C1 and C2 carbonaceous chondrites by stepped combustion. Meteorit. Planet. Sci. 26, 55–64.

Carporzen, L., Weiss, B.P., Elkins-Taton, L.T., Shuster, D.L., Ebel, D., Gattacceca, J., 2011. Magnetic evidence for a partially differentiated carbonaceous chondrite parent body. Proc. Natl. Acad. Sci. USA 108, 6386–6389.

Chizmadia, L.J., Brearley, A.J., 2008. Mineralogy, aqueous alteration, and primitive textural characteristics of fine-grained rims in the Y-791198 CM2 carbonaceous chondrite: TEM observations and comparison to ALHA81002. Geochim. Cosmochim. Acta 72, 602–625.

Clayton, R.N., Onuma, N., Mayeda, T.K., 1976. A classification of meteorites based on oxygen isotopes. Earth Planet. Sci. Lett. 30, 10–18.

Clayton, R.N., Onuma, N., Grossman, L., Mayeda, T.K., 1977. Distribution of the presolar component in Allende and other carbonaceous chondrites. Earth Planet. Sci. Lett. 34, 209–224.

Cody, G.D., Alexander, C.M.O'D., Yabuta, H., Kilcoyne, A.L.D., Araki, T., Ade, H., Dera, P., Fogel, M., Militzer, B., Mysen, B.O., 2008. Organic thermometry for chondritic parent bodies. Earth Planet. Sci. Lett. 272, 446–455.

Crutcher, R.M., 2012. Magnetic fields in molecular clouds. Annu. Rev. Astron. Astrophys. 50, 29–63.

Day, R., Fuller, M., Schmidt, V.A., 1977. Hysteresis properties of titanomagnetites: grain size and composition dependence. Phys. Earth Planet. Inter. 13, 260–267.

De Leuw, S., Rubin, A.E., Schmitt, A.K., Wasson, J.T., 2009. ^{53}Mn–^{53}Cr systematics of carbonates in CM chondrites: implications for the timing and duration of aqueous alteration. Geochim. Cosmochim. Acta 73, 7433–7442.

Dunlop, D.J., Ozdemir, O., Clark, D.A., Schmidt, P.W., 2000. Time–temperature relations for the remagnetization of pyrrhotite (Fe_7S_8) and their use in estimating paleotemperatures. Earth Planet. Sci. Lett. 176, 107–116.

Elkins-Tanton, L.T., Weiss, B.P., Zuber, M.T., 2011. Chondrites as samples of differentiated planetesimals. Earth Planet. Sci. Lett. 305, 1–10.

Elmaleh, A., Tarantino, S.C., Zema, M., Devouard, B., Fialin, M., 2012. The low-temperature magnetic signature of Fe-rich serpentine in CM2 chondrites: comparison with terrestrial cronstedtite and evolution with the degree of alteration. Geochem. Geophys. Geosyst. 13, 5, Q05Z42.

Enkin, R.J., Dunlop, D.J., 1988. The demagnetization temperature necessary to remove viscous remanent magnetization. Geophys. Res. Lett. 15, 514–517.

Eugster, O., Herzog, G.F., Marti, K., Caffee, M.W., 2006. Irradiation records, cosmic-ray exposure ages, and transfer times of meteorites. In: Lauretta, D., McSween Jr., H.Y. (Eds.), Meteorites and the Early Solar System, vol. II. Arizona University Press, pp. 829–851.

Farinella, P., Froeschlé, Ch., Gonczi, R., Hahn, G., Morbidelli, A., Valsecchi, G.B., 1994. Asteroids falling onto the Sun. Nature 371, 315–317.

Fu, R.R., Elkins-Tanton, L., 2014. The fate of magmas in planetesimals and the retention of primitive chondritic crusts. Earth Planet. Sci. Lett. 390, 128–137.

Fu, R.R., Weiss, B.P., 2012. Detrital remanent magnetization in the solar nebula. J. Geophys. Res., Planets 117 (E2).

Fu, R.R., Weiss, B.P., Shuster, D.L., Gattacceca, J., Grove, T.L., Suavet, C., Lima, E.A., Li, L., Kuan, A.T., 2012. An ancient core dynamo in asteroid Vesta. Science 338, 238–241.

Fujiya, W., Sugiura, N., Hotta, H., Ichimura, K., Sano, Y., 2012. Evidence for the late formation of hydrous asteroids from young meteoritic carbonates. Nat. Commun. 3, 627.

Gambino, R.J., McGuire, T.R., Nakamura, Y., 1967. Magnetic properties of the iron-group metal phosphides. J. Appl. Phys. 38, 1253.

Gammie, C.F., 1996. Layered accretion in T Tauri disks. Astrophys. J. 457, 355–362.

Gattacceca, J., Rochette, P., 2002. Pseudopaleosecular variation due to remanence anisotropy in a pyroclastic flow succession. Geophys. Res. Lett. 29. 126-1-4.

Gattacceca, J., Rochette, P., 2004. Toward a robust normalized magnetic paleointensity method applied to meteorites. Earth Planet. Sci. Lett. 227, 377–393.

Gattacceca, J., Rochette, P., Denise, M., Consolmagno, G., Folco, L., 2005. An impact origin for the foliations of chondrites. Earth Planet. Sci. Lett. 234, 351–368.

Gattacceca, J., Boustie, M., Hood, L., Cuq-Lelandais, J.-P., Fuller, M., Bezaeva, N.S., 2010. Can the lunar crust be magnetized by shock: experimental ground truth. Earth Planet. Sci. Lett. 299, 42–53.

Gladman, B.J., Migliorini, F., Morbidelli, A., Zappalà, V., Michel, P., Cellino, A., Froeschlé, C., Levison, H.F., Bailey, M., Duncan, M., 1997. Dynamical lifetime of objects injected into asteroid belt resonances. Science 277, 197.

Gounelle, M., Engrand, C., Alard, O., Bland, P.A., Zolensky, M.E., Russell, S.S., Duprat, J., 2005a. The hydrogen isotopic composition of water from fossil micrometeorites. Geochim. Cosmochim. Acta 69, 3431–3443.

Gounelle, M., Engrand, C., Maurette, M., Kurat, G., McKeegan, K.D., Brandstätter, F., 2005b. Small Antarctic micrometeorites (25–50 μm): a mineralogical and in situ oxygen isotopes study. Meteorit. Planet. Sci. 40, 917–932.

Gounelle, M., Morbidelli, A., Bland, P.A., Sephton, M.A., Young, E.D., Spurny, P., 2008. Meteorites from the outer solar system? In: Barucci, A., Boehnhardt, H., Cruikshank, D., Morbidelli, A. (Eds.), The Solar System Beyond Neptune. Arizona University Press, pp. 525–541. Tucson. Lett. 3, 351–354.

Grady, M.M., 2000. Catalogue of Meteorites, 5th ed. Cambridge University Press. 689 pp.

Grimm, R.E., McSween Jr., H.Y., 1989. Water and the thermal evolution of carbonaceous chondrite parent bodies. Icarus 82, 244–280.

Guo, W., Eiler, J.M., 2007. Temperatures of aqueous alteration and evidence for methane generation on the parent bodies of CM chondrites. Geochim. Cosmochim. Acta 71, 5565–5575.

Haack, H., Michelsen, R., Stober, G., Keuer, D., Singer, W., Williams, I., 2011. CM chondrites from comets?—New constraints from the orbit of the Maribo CM chondrite fall. Formation of the First Solids in the Solar System, (abstract) 9100.

Hanowski, N.P., Brearley, A.J., 2000. Iron-rich aureoles in the CM carbonaceous chondrites, Murray, Murchison, and Allan Hills 81002; evidence for in-situ aqueous alteration. Meteorit. Planet. Sci. 35, 1291–1308.

Hanowski, N.P., Brearley, A.J., 2001. Aqueous alteration of chondrules in the CM carbonaceous chondrite, Allan Hills 81002: implications for parent body alteration. Geochim. Cosmochim. Acta 65, 495–518.

Harries, D., Langenhorst, F., 2013. The nanoscale mineralogy of the Fe, Ni sulfides in pristine and metamorphosed CM and CM/CI-like chondrites: tapping a petrogenetic record. Meteorit. Planet. Sci. 48, 879–903.

Hewins, R.H., Bourot-Denise, M., Zanda, B., Leroux, H., Barrat, J.-A., Humayun, M., Göpel, C., Greenwood, R.C., Franchi, I.A., Pont, S., Lorand, J.-P., Cournède, C., Gattacceca, J., Rochette, P., Kuga, M., Marrocchi, Y., Marty, B., 2014. The Paris meteorite, the least altered CM chondrite so far. Geochim. Cosmochim. Acta 124, 190–222.

Howard, K.T., Benedix, G.K., Bland, P.A., Cressey, G., 2009. Modal mineralogy of CM2 chondrites by X-ray diffraction (PSD-XRD): Part 1. Total phyllosillicate abundance and the degree of aqueous alteration. Geochim. Cosmochim. Acta 73, 4576–4589.

Howard, K.T., Benedix, G.K., Bland, P.A., Cressey, G., 2011. Modal mineralogy of CM chondrites by X-ray diffraction (PSD-XRD): Part 2. Degree, nature and settings of aqueous alteration. Geochim. Cosmochim. Acta 75, 2735–2751.

Hyman, M., Rowe, M.W., 1983. The origin of magnetite in carbonaceous chondrites. Lunar Planet. Inst. 14, 341–342.

Hyman, M., Rowe, M.W., 1986. Saturation magnetization measurements of carbonaceous chondrites. Meteoritics 21 (1), 1–22.

Jelinek, V., 1981. Characterization of the magnetic fabric of rocks. Tectonophysics 79, 63–67.

Jenniskens, P., 69 co-authors, 2012. Radar enabled recovery of the Sutter's Mill meteorite, a carbonaceous chondrite regolith breccia. Science 338, 1583–1587.

Kebukawa, Y., Nakashima, S., Zolensky, M.E., 2010. Kinetic of organic matter degradation in the Murchison meteorite for the evaluation of parent-body temperature history. Meteorit. Planet. Sci. 45 (1), 99–113.

Kimura, M., Grossman, J.N., Weisberg, M.K., 2011. Fe–Ni metal and sulfide mineral in CM chondrites: an indicator of thermal history. Meteorit. Planet. Sci. 46 (3), 431–442.

Kirschvink, J.L., 1980. The least-squares line and plane and the analysis of palaeomagnetic data. Geophys. J. Int. 62, 699–718.

Kleine, T., Munker, C., Mezger, K., Palme, H., 2002. Rapid accretion and early core formation on asteroids and the terrestrial planets from Hf–W chronometry. Nature 418, 952–955.

Kletetschka, G., Kohout, T., Wasilewski, P.J., 2003. Magnetic remanence in the Murchison meteorite. Meteorit. Planet. Sci. 38 (3), 399–405.

Kruijer, T.S., Sprung, P., Kleine, T., Leya, I., Burkhardt, C., Wieler, R., 2012. Hf–W chronometry of core formation in planetesimals inferred from weakly irradiated iron meteorites. Geochim. Cosmochim. Acta 99, 287–304.

Larson, E.E., Watson, D.E., Herndon, J.M., Rowe, M.W., 1973. Partial A.F. demagnetization studies of 40 meteorites. J. Geomagn. Geoelectr. 25, 331–338.

Lauretta, D.S., Hua, X., Buseck, P.R., 2000. Mineralogy of fine-grained rims in the ALH 81002 CM chondrite. Geochim. Cosmochim. Acta 64, 3263–3273.

Lindgren, P., Hanna, R.D., Dobson, K.J., Tomkinson, T., Lee, M.R., in press. The paradox between low shock-stage and evidence for compaction in CM carbonaceous chondrites explained by multiple low-intensity impacts. Geochim. Cosmochim. Acta. http://dx.doi.org/10.1016/j.gca.2014.09.014.

Mason, B., 1962. The carbonaceous chondrites. Space Sci. Rev. 1, 621–646.

McClelland, E., 1996. Theory of CRM acquired by grain growth, and its implications for TRM discrimination and paleointensity determination in igneous rocks. Geophys. J. Int. 126, 271–280.

McSween, H.Y., 1979. Alteration in CM carbonaceous chondrites inferred from modal and chemical variation in matrix. Geochim. Cosmochim. Acta 43, 1761–1770.

Metzler, K., Bischoff, A., Stöffler, D., 1992. Accretionary dust mantles in CM chondrites: evidence for solar nebula processes. Geochim. Cosmochim. Acta 56, 2873–2897.

Morbidelli, A., Gounelle, M., Levison, H.F., Bottke, W.F., 2006. Formation of the binary near-Earth object 1996 FG3: can binary NEOs be the source of short-CRE meteorites? Meteorit. Planet. Sci. 41, 875–887.

Nakato, A., Brearley, A.J., Nakamura, T., Noguchi, T., Ahn, I., Lee, J.I., Matsuoka, M., Sasaki, S., 2013. Diversity of thermal evolution processes in the hydrous asteroids identified in thermally metamorphosed carbonaceous chondrites PCA02012. 76th Annual Meteoritical Society Meeting. Abstract 5282.

Nazarov, M.A., Kurat, G., Brandstätter, F., Ntaflos, T., Chaussidon, M., Hoppe, P., 2009. Phosphorus-bearing sulfides and their associations in CM chondrites. Petrology 17 (2), 101–123.

Nishiizumi, K., Arnold, J.R., Caffee, M.W., Finkel, R.C., Southon, J.R., Nagai, H., Honda, M., Imamura, M., Kobayashi, K., Sharma, P., 1993. Exposure ages of carbonaceous chondrites. Lunar Planet. Sci. Conf. Abstr. 24. Abstract #1085.

Pullaiha, G., Irving, E., Buchan, K.L., Dunlop, D.J., 1975. Magnetization changes caused by burial and uplift. Earth Planet. Sci. Lett. 28, 133–143.

Pravdivtseva, O., Meshik, A., Hohenberg, C.M., 2013. The I–Xe record: early onset of aqueous alteration in magnetites separated from CM and CV carbonaceous chondrites. Lunar Planet. Sci. Conf. Abstr. 44. Abstract #3104.

Redmer, R., Mattsson, T.R., Nettelmann, N., French, M., 2011. The phase diagram of water and the magnetic fields of Uranus and Neptune. Icarus 211, 798–803.

Rochette, P., Fillion, G., Matteí, J.L., Dekkers, M.J., 1990. Magnetic transition at 30–34 K in pyrrhotite: insight into a widespread occurrence of this mineral in rocks. Earth Planet. Sci. Lett. 98, 319–328.

Rochette, P., Gattacceca, J., Bonal, L., Bourot-Denise, M., Chevrier, V., Clerc, J.P., Consolmagno, G., Folco, L., Gounelle, M., Kohout, T., Pesonen, L.J., Quirico, E., Sagnotti, L., Skripnik, A., 2008. Magnetic classification of stony meteorites: 2. Non-ordinary chondrites. Meteorit. Planet. Sci. 43, 959–980.

Rosenberg, N.D., Browning, L., Bourcier, W.L., 2001. Modeling aqueous alteration of CM carbonaceous chondrites. Meteorit. Planet. Sci. 36, 239–244.

Rubin, A.E., 2012. Collisional facilitation of aqueous alteration of CM and CV carbonaceous chondrites. Geochim. Cosmochim. Acta 90, 181–194.

Rubin, A.E., Wasson, J.T., 1986. Chondrules in the Murray CM2 meteorite and compositional differences between CM-CO and ordinary chondrite chondrules. Geochim. Cosmochim. Acta 50, 307–315.

Rubin, A.E., Trigo-Rodriguez, J.M., Huber, H., Wasson, J.T., 2007. Progressive aqueous alteration of CM carbonaceous chondrites. Geochim. Cosmochim. Acta 71, 2361–2382.

Scott, E.R.D., Keil, K., Stoffler, D., 1992. Shock metamorphism of carbonaceous chondrites. Geochim. Cosmochim. Acta 56, 4281–4293.

Sears, D.W., 1975. Temperature gradients in meteorites produced by heating during atmospheric passage. Mod. Geol. 5, 155–164.

Spencer, J.R., Lebofsky, L.A., Sykes, M.V., 1989. Systematic biases in radiometric diameter determinations. Icarus 78, 337–354.

Stephenson, A., Collinson, D.W., 1974. Lunar magnetic field paleointensities determined by an anhysteretic remanent magnetization method. Earth Planet. Sci. Lett. 23, 220–228.

Tarduno, J.A., Cottrell, R.D., Nimmo, F., Hopkins, J., Voronov, J., et al., 2012. Evidence for a dynamo in the main group pallasite parent body. Science 338, 939–942.

Tomeoka, K., McSween, H.Y., Buseck, P.R., 1989. Mineralogical alteration of CM carbonaceous chondrites: a review. Proc. NIPR Symp. Antarct. Meteor. 2, 221–234.

Turner, N.J., Sano, T., 2008. Dead zone accretion flows in protostellar disks. Astrophys. J. 679, L131, 4 pp.

Wasilewski, P., Acuna, M.H., Kletetschka, G., 2002. 433 Eros: problems with the meteorite magnetism record in attempting an asteroid match. Meteorit. Planet. Sci. 37, 937–950.

Wasson, J.T., 1976. Relative abundance of CM chondrites in the inner and outer solar system. Meteoritics 11, 385.

Wasson, J.T., Wetherill, G.W., 1979. Dynamical, chemical and isotopic evidence regarding the formation locations of asteroids and meteorites. In: Gehrels, T. (Ed.), Asteroids. The University of Arizona Press, pp. 926–974.

Weiss, B.P., Elkins-Tanton, L.T., 2013. Differentiation planetesimals and the parent bodies of chondrites. Annu. Rev. Earth Planet. Sci. 41, 529–560.

Weiss, B.P., Berdahl, J.S., Elkins-Tanton, L., Stanley, S., Lima, E.A., Carpozen, L., 2008. Magnetism on the Angrite parent body and the early differentiation of planetesimals. Science 322, 713–716.

Weiss, B.P., Gattacceca, J., Stanley, S., Rochette, P., Christensen, U.R., 2010. Paleomagnetic records of meteorites and early planetesimal differentiation. Space Sci. Rev. 152, 341–390.

Wood, J.A., 1963. On the origin of chondrules and chondrites. Icarus 2, 152–180.

Young, E.D., Ash, R.D., England, P., Rumble III, D., 1999. Fluid flow in chondritic parent bodies: deciphering the compositions of planetesimal. Science 286, 1331.

Zanda, B., Bourot-Denise, M., Hewins, R.H., Barrat, J.-A., Gattacceca, J., 2010. The Paris CM chondrite yields new insights on the onset of parent body alteration. In: 73rd Annual Meteoritical Society Meeting. Abstract #5312.

Zlotnicki, J., le Mouel, J.L., 1990. Possible electrokinetic origin of large magnetic variations at La-Fournaise volcano. Nature 343, 633–636.

Zolensky, M.E., McSween, H.Y., 1988. Aqueous alteration. In: Kerridge, J.F., Matthews, M.S. (Eds.), Meteorites and the Early Solar System. University of Arizona Press, pp. 114–143.